

Spatial heterogeneity of aftershock productivity on the Kumamoto earthquake rupture modeled by the finite source ETAS model

YICUN GUO リスク解析戦略研究センター 特任助教

[SUMMARY]

We proposed an extended version of the space-time ETAS model which simultaneously incorporates earthquake focal depths and rupture geometries of large earthquakes. This new model is applied to the 2016 Kumamoto earthquake sequence. The results show that the improved model corrects the biased estimation of model parameters due to the isotropic distribution of aftershocks in the point source ETAS model. The reconstructed patterns of aftershock productivity show significant migrations in space and time. In near field (10 km from areas with slips greater than 1 m), the decay of linear aftershock density follows an inverse power law of distance with an exponent -0.5 , which is consistent with the decay of aftershock density triggered by static stress changes. Through comparisons between our results and slip distributions, we find that high aftershock productivity forms complementary patterns for coseismic slips in space, indicating that aftershocks play a role in the postseismic relaxation process.

[Methodology]

The total seismicity function in the 3D-ETAS model is in the form of

$$\lambda(t, x, y, z | H_t) = \mu(x, y, z) + \sum_{i: t_i < t} \xi(t - t_i, x - x_i, y - y_i, z; M_i, z_i),$$

where $\mu(x, y, z)$ is the background seismicity rate assumed to be temporally stationary, and i runs over all the events in the observation history H_t .

The clustering seismicity rate is composed of four parts:

$$\xi(t, x, y, z; M, z') = \kappa(M)g(t)f(x, y; M)h(z, z').$$

They are direct aftershock productivity:

$$\kappa(M) = Ae^{\alpha(M-M_c)}, M \geq M_c;$$

the time probability density function (pdf; normalized Omori-Utsu law):

$$g(t) = \frac{p-1}{c} \left(1 + \frac{t}{c}\right)^{-p};$$

epicentre pdf:

$$f(x, y; M) = \frac{q-1}{\pi D^2 e^{\gamma(M-M_c)}} \left(1 + \frac{x^2 + y^2}{D^2 e^{\gamma(M-M_c)}}\right)^{-q}$$

and depth pdf:

$$h(z; z') = \frac{\left(\frac{z}{z'}\right)^{\eta z'/z} \left(1 - \frac{z}{z'}\right)^{\eta(1-z'/z)}}{Z B\left(\frac{\eta z'}{z} + 1, \eta\left(1 - \frac{z'}{z}\right) + 1\right)},$$

with Beta function:

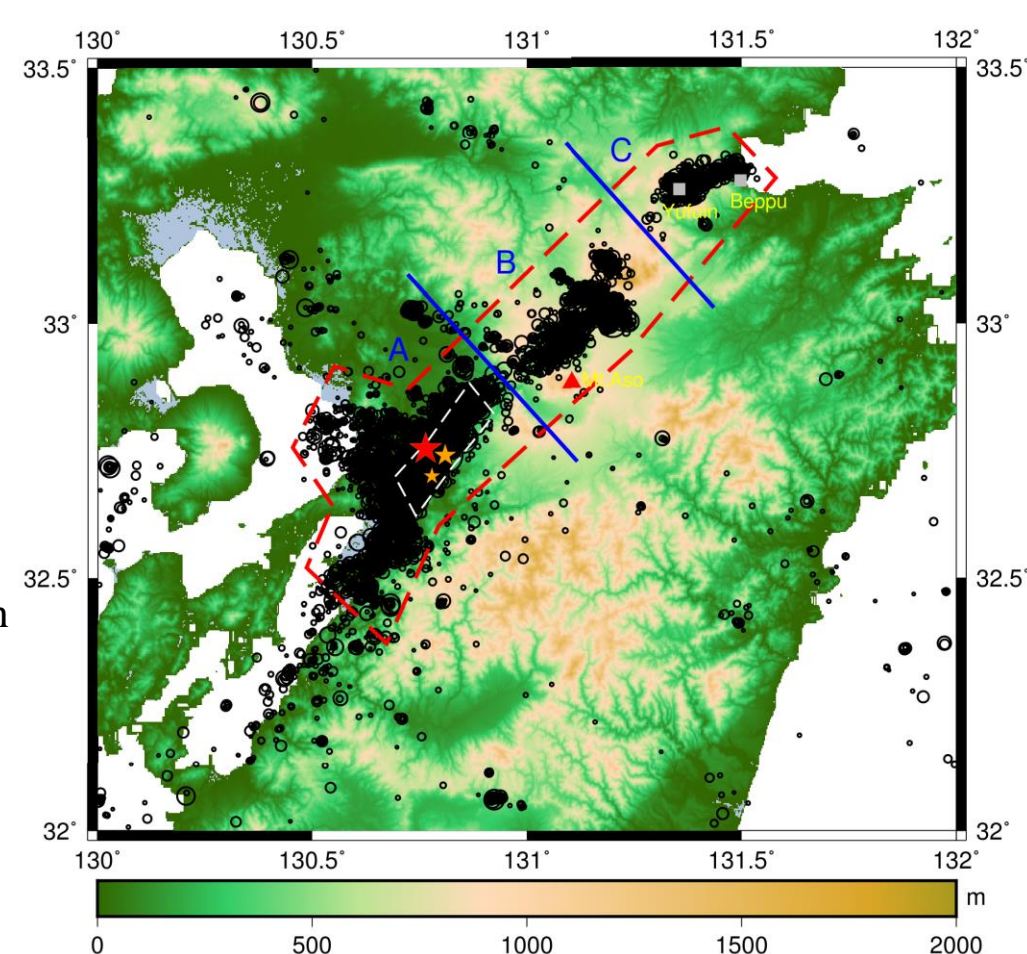
$$B(p, q) = \int_0^1 t^{p-1} (1-t)^{q-1} dt,$$

and finite source kernel for large earthquakes

$$f(x, y; S_i, M_i) = \frac{q-1}{\pi D'^2} \sum_{i=1}^{n_i} \frac{\tau_{ii}}{P_i} \left[1 + \frac{(x - u_{ii})^2 + (y - v_{ii})^2}{D'^2} \right]^{-q}$$

[Data]

Figure 1. (a) The epicenter distribution of earthquakes (black circles). The red and yellow pentagrams represent for the Kumamoto M7.3 mainshock on 15 April 2016 and the two M6.5 and M6.4 foreshocks on 14 April 2016, respectively. The red and white dash lines denote the source boundaries of the mainshock and two foreshocks, respectively.



[Reconstruction]

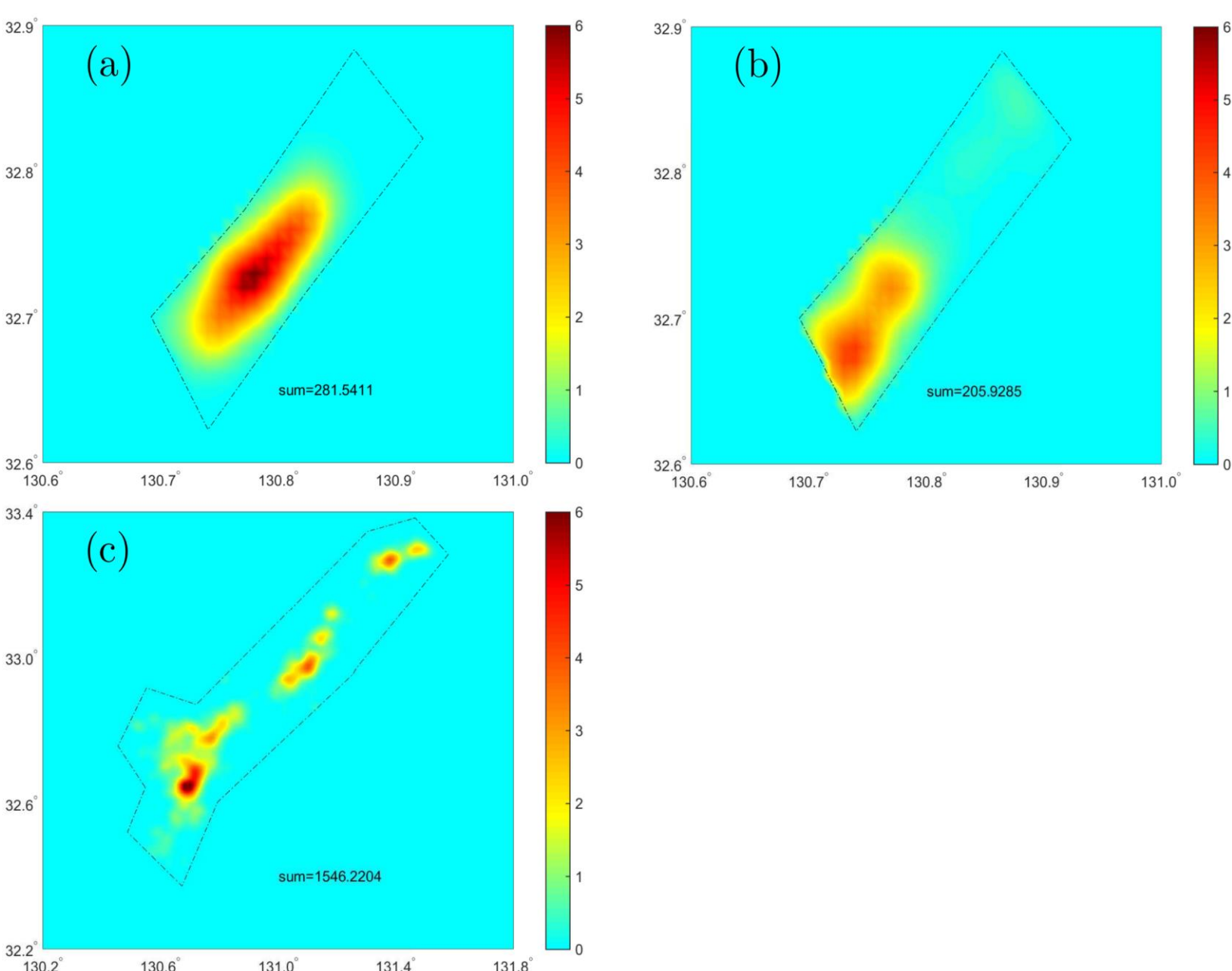


Figure 2. Reconstructed aftershock productivity patterns from the 2D finite source model. The sum in each panel represents the total productivity value.

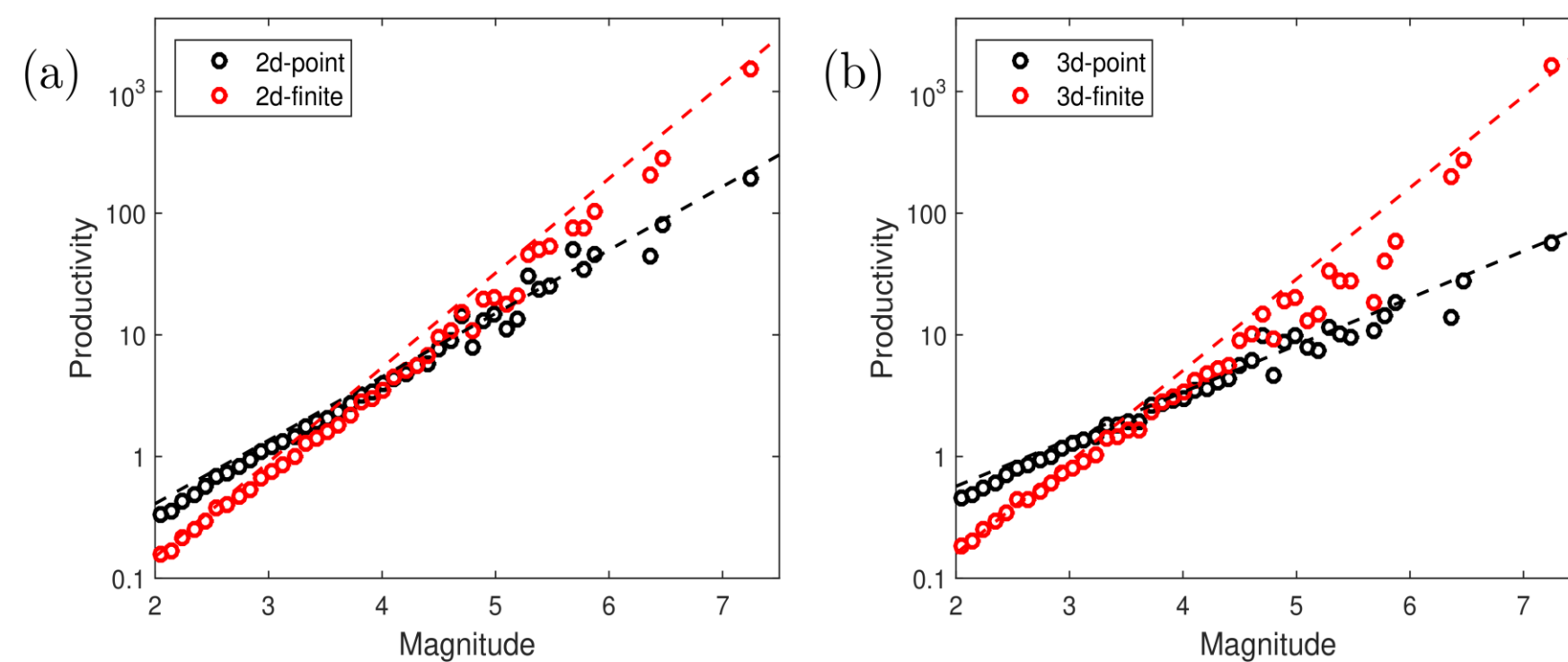


Figure 3. Reconstructed results of aftershock productivity versus magnitude. The red, black dash lines are theoretical lines in point and finite source models, respectively.

[Family Trees]

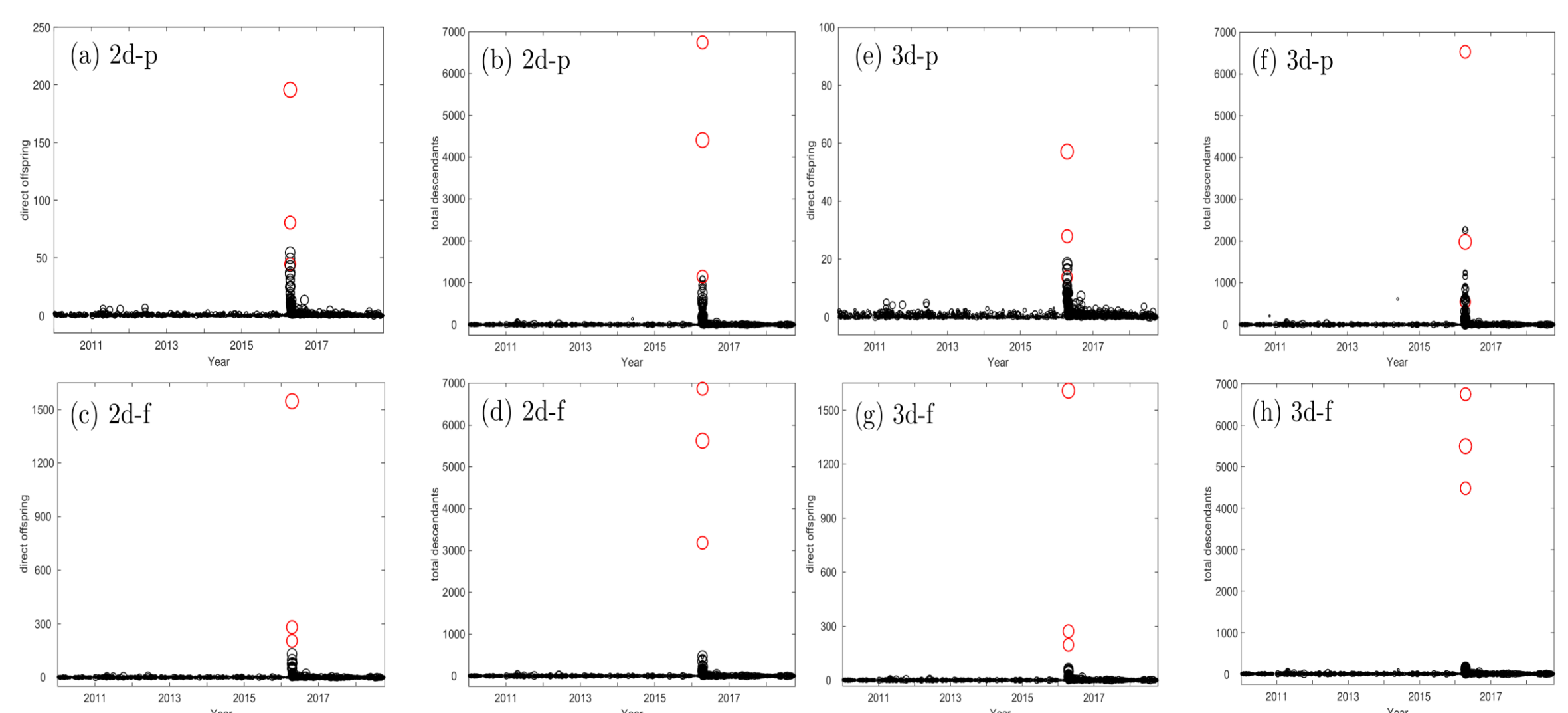


Figure 4. Estimated numbers of direct offspring and total descendants of all events versus their occurrence times. The size of circles represents for the magnitudes. Two foreshocks and the mainshock are marked in red circles.

[Aftershock Productivity]

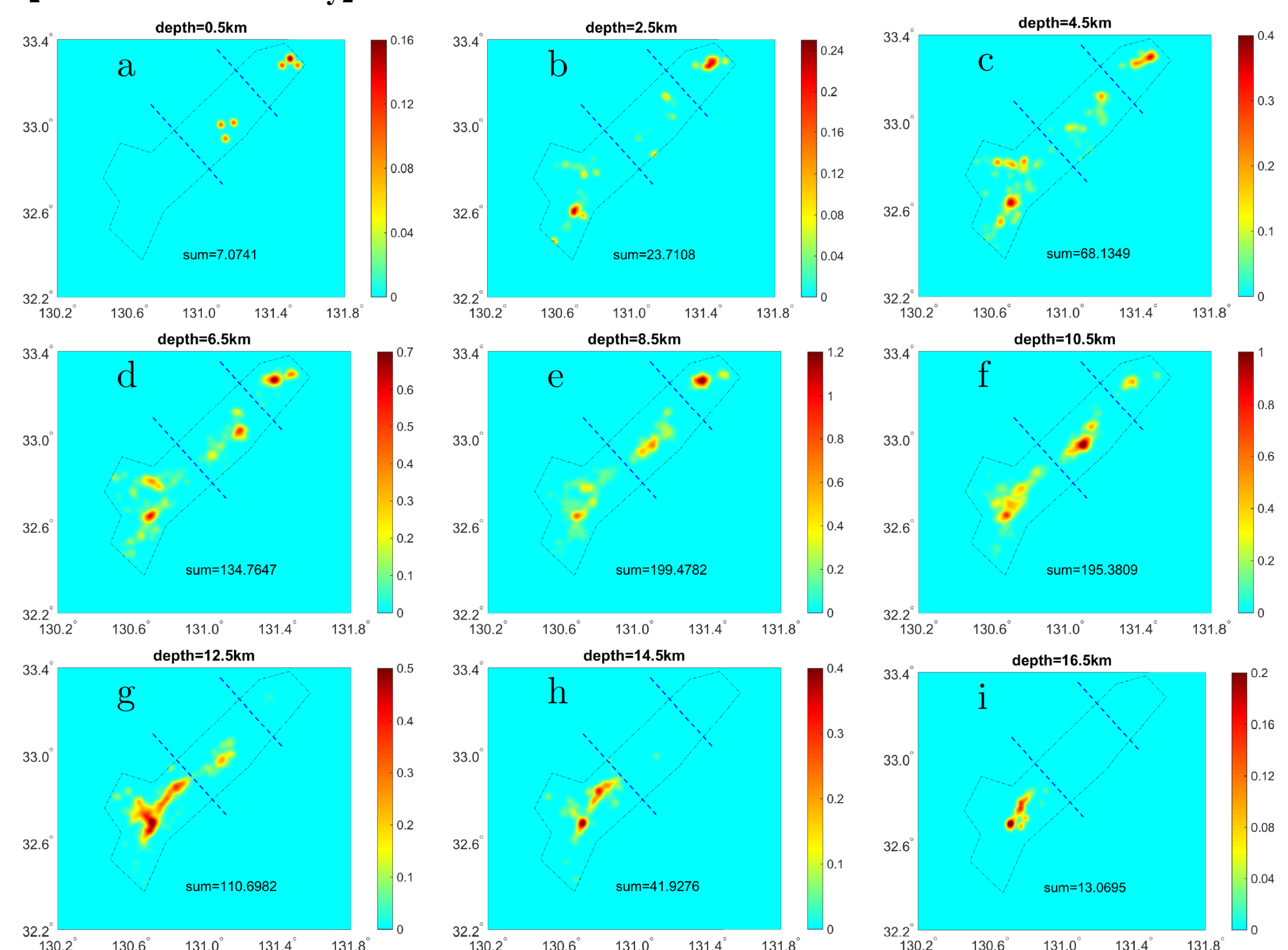


Figure 5. The productivity distribution of the mainshock at different depths. The total productivity of corresponding depth is summed up as the number in each panel.

[Conclusions]

We propose the 3D-finite source ETAS model which simultaneously incorporates focal depths and rupture geometries of large earthquakes.

The finite models correct the underestimated direct offspring of large earthquakes in point models.

The reconstructed patterns of aftershock productivity show significant migrations in space and time, indicating complicated postseismic stress adjustments.

Areas of high aftershock productivity form complementary patterns for coseismic slips, meaning that aftershocks contribute to the postseismic relaxation process.